Computational study of the structural phases of ZnO

Mahlaga P. Molepo* and Daniel P. Joubert
School of Physics, University of the Witwatersrand, Private Bag X3, Wits 2050, Johannesburg, South Africa
(Received 5 October 2010; revised manuscript received 14 July 2011; published 19 September 2011)

We use first-principles calculations based on density functional theory to study the structural properties and pressure-induced solid-solid phase transitions of ZnO. Both the local-density and the generalized gradient approximations are employed together with the projector augmented wave potentials to mimic the electron-ion interaction. We consider the wurtzite (B4), rocksalt (B1), zinc blende (B3), CsCl (B2), NaTl (B32), WC (B_h), BN (B_k), NiAs ($B8_1$), and AsTi (B_i) modifications of ZnO. The calculated structural properties in the B4, B3, B1, and B2 phases are in excellent agreement with earlier *ab initio* predictions, as is the transition pressure between them. We find that the B4 phase is the most preferred low-pressure candidate in ZnO while the B2 phase is favorable at high pressures. Apart from the previously reported $B4 \rightarrow B1 \rightarrow B2$ phase transition, our study reveals other possible paths for a transition from the B4 to the B2 phase.

DOI: 10.1103/PhysRevB.84.094110 PACS number(s): 61.50.Ks, 81.40.Vw, 64.70.K−, 71.20.Ps

I. INTRODUCTION

Zinc oxide (ZnO) is a group IIB-VIA semiconductor with a variety of technological applications including thin film-based electronic and electro-optic devices, varistors, and conductive solar cell window layers. Due to its importance in various application domains, the properties of ZnO have been the subject of several theoretical and experimental investigations.[1-4] Its structural and electronic properties are, in particular, important for applications such as chemical sensors in gas detecting systems and catalysts for hydrogenation and dehydrogenation reactions.[5] There is also a continuing interest in the high-pressure behavior of ZnO in the areas of geophysics and fundamental materials physics.[6] It occurs naturally as a mineral and its high-pressure phase may be geologically important as a component of the lower mantle.[7]

Contrary to other IIB-VIA binary compounds which adopt different metastable structures, bulk ZnO is known to crystallize only in the hexagonal wurtzite (B4) structure under normal conditions. A number of experiments[1-3] have shown through different techniques that the B4 structure transforms into a cubic rocksalt (B1) structure at a pressure in the vicinity of 9 GPa. A recent angular dispersive x-ray diffraction experiment by Liu *et al.*[8] has shown that the B1 phase of ZnO remains stable under high pressure up to 209 GPa at room temperature, being the maximum pressure achieved in any experiment on ZnO so far.

With recent progress in computational strategy and performance, computer simulations are increasingly used by theorists to understand properties of matter and make specific predictions for real materials and experimentally observable phenomena. This has been exploited by *ab initio* (first principles) simulations, using the local density[9] and generalized gradient[10] approximations (LDA and GGA) of density functional theory[9,11] (DFT). The advent of DFT and the invention of *ab initio* pseudopotentials have made it feasible to calculate, with a fair level of accuracy, ground state structural and electronic properties, as well as to predict stabilities of crystalline phases in real solids. Over the past two decades, these theoretical approaches have been used to study the phase transitions in ZnO. It has been reported[4,6,12-14] that at pressures around 260 GPa, ZnO undergoes a phase transition from the B1 to the eightfold-coordinated B2 (cubic CsCl) structure, assuming that no other structures appear first. These studies were based on the widely used DFT within LDA and GGA together with Gaussian basis sets, and were expected to stimulate corresponding high-pressure experimental work. On the other hand, an atomistic calculation performed by Zaoui and Sekkal[15] predicted the transition at 305 GPa. However, most of the previous studies on high-pressure behavior of ZnO did not consider any other possible structures, except B4, B3 (cubic zinc blende), B1, and B2. Recently, Azzaz *et al.*[16] investigated the ground-state properties of ZnO on other structures such as cinnabar, d-β-tin, and NiAs. First principles lattice dynamics calculation by Li *et al.*[17] also predicted a high-pressure tetragonal PbO-type (B10) structure as an intermediate phase between the B1 and the hypothetical B2 phase.

In this work, we perform first principles electronic structure calculations for nine different structures of ZnO. We consider the NaTl (B32), WC (B_h), BN (B_k), NiAs ($B8_1$), and AsTi (B_i) modifications in addition to the most studied four structures. These structures are chosen in order to check if they could be potential candidates for the most stable phase at high pressure. The objective is to predict the equilibrium structural and electronic properties including lattice parameters, bulk moduli and stabilities for these structures. We also predict the phase transitions between the structures and construct a detailed structural phase diagram for ZnO.

II. COMPUTATIONAL DETAILS

First-principles calculations were performed using the Vienna *ab initio* simulation package (VASP)[18,19] based on density functional theory.[11] The electronic exchange-correlation interactions are treated by the LDA in the scheme of Ceperly and Alder[20] as parameterized by Perdew and Zunger,[21] and the GGA of Perdew, Burke and Ernzerhof[10] (PBE96). The interaction between ions and valence electrons is described by the projector-augmented wave (PAW) potential method.[22,23] The one-electron pseudo-orbitals are expanded over a planewave basis set that includes all plane waves whose kinetic energy $\hbar^2k^2/2m < E_{\text{cut}}$ where k is the wave vector, m the electron mass, and E_{cut} the chosen cutoff energy. For all calculations

TABLE I. Equilibrium structural properties for nine phases of ZnO calculated with LDA and GGA (values in brackets) functionals.

	a_0 (Å)	c_0(Å)	B_0 (GPa)
B4 (wurtzite)	3.209 (3.302)	5.128 (5.275)	159.4 (127.5)
Exp.	3.2498[a]	5.2066[a], 5.2042[b]	142.6[a]
	3.2496[b]		183.0[b]
Theory	3.205[c] (3.295)[c]		155[c] (124)[c]
	(3.2819)[d]	(5.3264)[d]	(129.19)[d]
B3 (zinc blende)	4.505 (4.634)		161.1 (129.3)
Theory	4.509[c] (4.637)[c]		154[c] (124)[c]
	(4.6329)[d]		(139.32)[d]
B2 (CsCl)	2.618 (2.693)		202.2 (159.5)
Theory	2.614[c] (2.689)[c]		201[c] (161)[c]
	(2.6680)[d]		(159.91)[d]
B1 (rocksalt)	4.224 (4.340)		204.9 (163.4)
Exp.	4.283[a]		202.5[a], 228[b]
	4.271[b]		
Theory	4.218[c] (4.334)[c]		203[c] (163)[c]
	(4.3379)[d]		(164.91)[d]
B32 (NaTl)	5.391 (5.565)		159.9 (121.1)
B_h (WC)	2.943 (3.025)	2.549 (2.618)	190.1 (149.9)
B_k (BN)	3.161 (3.240)	5.165 (5.294)	143.7 (127.4)
$B8_1$ (NiAs)	2.975 (3.051)	4.971 (5.135)	199.8 (157.2)
Theory	3.10[e]		202.50[e]
B_i (AsTi)	2.953 (3.025)	4.970 (5.103)	246.9 (198.3)

[a]Reference 3.
[b]Reference 2.
[c]Reference 12.
[d]Reference 4.
[e]Reference 16.

reported in this work, the basis set contains planewaves up to energy cutoff of 400 eV.

Large sets of Monkhorst-Pack grids,[24] such as $14 \times 14 \times 8$, $19 \times 19 \times 19$, $12 \times 12 \times 12$, and $16 \times 16 \times 16$ for B4, B3, B1, and B2 structures respectively, were used to sample the Brillouin zone. These correspond to 120, 220, 182, and 120 k points in the irreducible part of the Brillouin zone. For the B_h, B_k, $B8_1$, and B_i modifications of a $9 \times 9 \times 6$ grid with 48 k points was used. The chosen planewave cutoff and the number of k points allow a convergence of the total energy to within 1 meV/atom. We have also used the Tetrahedron method with Blöchl corrections to improve convergence with respect to the number of k points. This method converges rapidly with the number of k points and does not require any empirical parameters, and is known to yield highly accurate results for bulk materials.[25]

III. STRUCTURAL PROPERTIES

Calculations of the total energy of ZnO were performed for each of the structures over a set of different unit cell volumes. Equilibrium structural properties were computed by fitting the total energy versus volume data to third-order Birch-Murnaghan isothermal equation of state function.[26] The calculated equilibrium volume V_0, lattice parameters, and the bulk modulus B_0 from the EOS are summarized in Table I, with GGA values shown inside brackets.

No experimental data is available, except for the B4 and B1 structures. For these structures we find LDA underestimates lattice parameters and atomic volumes compared to experiment, while the GGA overestimates them. This is a well-known feature of the local density versus generalized gradient approximations. We find a striking agreement between our LDA and GGA lattice parameters and bulk moduli values for the B4, B3, B1, and B2 phases and the corresponding values reported by Uddin and Scuseria,[12] obtained using Gaussian-type orbitals basis sets. Smaller differences can be attributed to pseudopotentials, basis sets, and other approximations intrinsic to a particular methodology. The GGA is seen to decrease the moduli compared to LDA. This softening is consistent with a weaker bonding shown by larger lattice parameters and atomic volumes. The B_i structure has the highest bulk modulus in both LDA and GGA. Therefore, we can expect that this phase should exhibit higher hardness than the other ZnO phases, assuming that hardness scales with the bulk modulus.

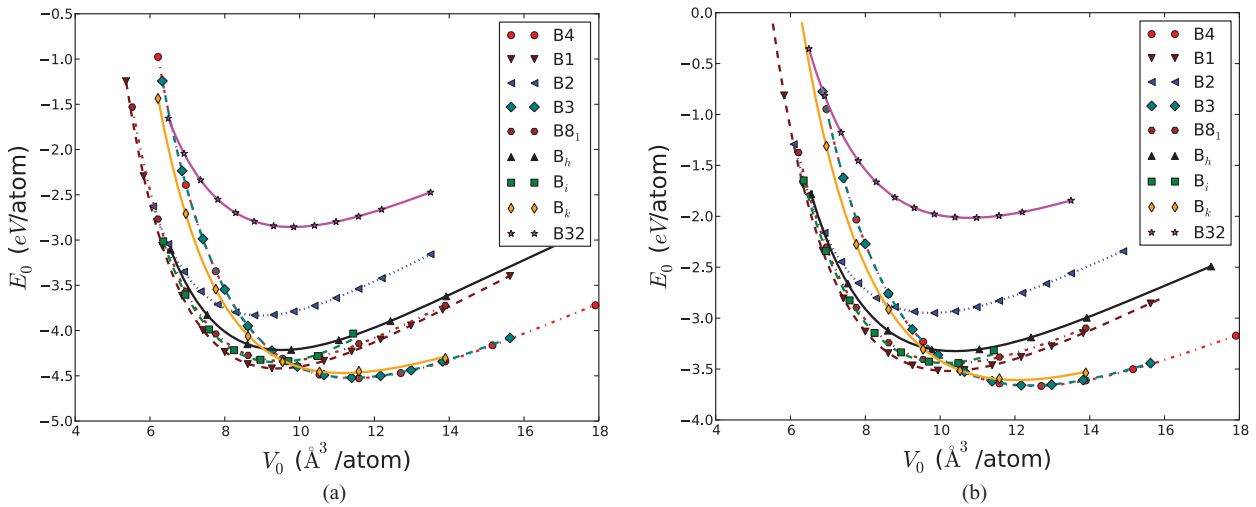

FIG. 1. (Color online) Energy (eV/atom) versus volume (Å^3/atom) for the phases of ZnO calculated with the (a) LDA and (b) PBE-GGA functionals. The curves are obtained using the third-order Birch-Murnaghan equation of states.

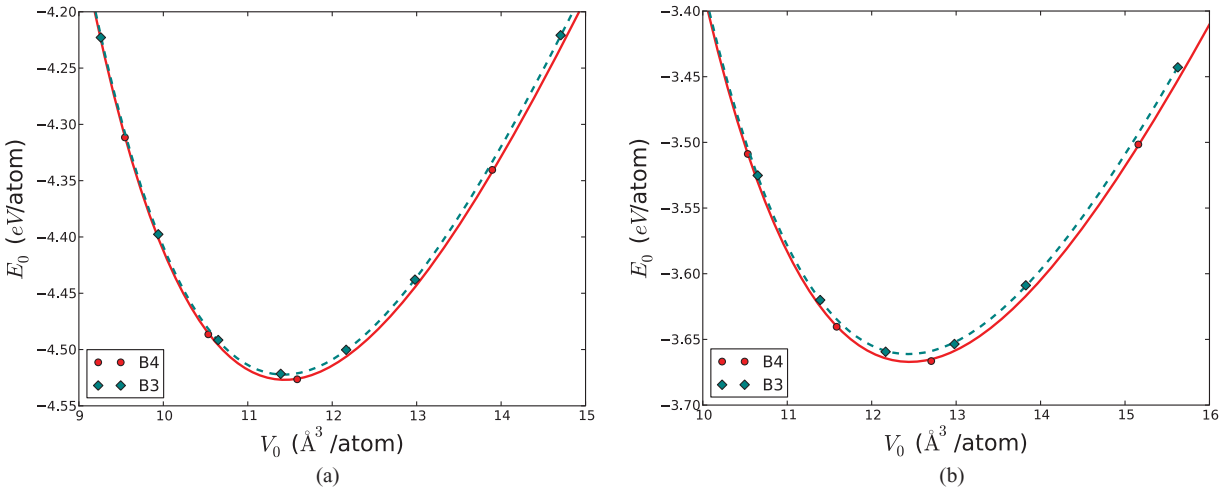

FIG. 2. (Color online) Energy (eV/atom) versus volume (Å^3/atom) for the wurtzite (B4) [solid curve] and zinc blende (B3) [dashed curve] phases of ZnO calculated with the (a) LDA and (b) PBE-GGA functionals. B4 is the lowest energy structure, hence the most stable phase at equilibrium.

IV. PHASE STABILITY

Energy versus volume calculations give an indication of which of the structures are the best candidates for the most stable phase. Generally, the structure with the lowest equilibrium energy is considered to be the most stable phase. In Fig. 1, we show the energy versus volume curves for ZnO calculated using the PAW method within the LDA and PBE-GGA functionals. The solid curves were obtained from the third-order Birch-Murnaghan EOS fitting.

From the curves it can be noted that the zinc blende (B3) and wurtzite (B4) phases have almost identical stabilities. In order to show the difference in the stability of the B4 and B3 structures, we show plots of their energy minima in Fig. 2 for both the LDA and GGA functionals. In both cases, it can be seen that the B4 phase is the most stable at zero temperature and pressure. This behavior has been observed in earlier studies of ZnO,[6,12,27] as well as in CdO by Moreno and Takechi,[28] and later in MgO by Schleife *et al.*[29] The B4 and B3 structures have the same local tetrahedral bonding geometry, but they

TABLE II. Calculated equilibrium structural volumes and cohesive energy for various phases of ZnO.

	This work		Other calculations	
	LDA	GGA	LDA	GGA
B4 (wurtzite)				
E_{coh} (eV)	9.063	7.337	9.769[a]	7.692[a],8.835[b]
V_0 (Å^3)	22.8	24.90	22.874[a]	24.834[a],24.906[b]
B3 (ZnS)				
E_{coh} (eV)	9.043	7.317	9.754[a]	7.679[a],8.768[b]
V_0 (Å^3)	22.86	24.86	22.914[a]	24.854[a],24.878[b]
B_k (BN)				
E_{coh} (eV)	8.962	7.216		
V_0 (Å^3)	22.36	24.08		
B1(rocksalt)				
E_{coh} (eV)	8.843	7.037	9.611[a]	7.455[a],8.489[b]
V_0 (Å^3)	18.84	20.46	18.904[a]	20.502[a],20.472[b]
B_i (AsTi)				
E_{coh} (eV)	8.703	6.878		
V_0 (Å^3)	18.76	20.22		
$B8_1$ (NiAs)				
E_{coh} (eV)	8.684	6.876		
V_0 (Å^3)	19.06	20.70	19.18[c]	
B_h (WC)				
E_{coh} (eV)	8.423	6.657		
V_0 (Å^3)	19.10	20.76		
B2 (CsCl)				
E_{coh} (eV)	7.663	5.895	8.462[a]	6.337[a],7.357[b]
V_0 (Å^3)	17.94	19.54	18.073[a]	19.785[a],19.581[b]
B32 (NaTl)				
E_{coh} (eV)	5.772	4.037		
V_0 (Å^3)	19.58	21.54		

[a]Reference 6.
[b]Reference 31.
[c]Reference 16.

TABLE III. Phase transition pressures (GPa) of ZnO obtained by common tangent method. Values from the enthalpy curve crossings are shown in brackets.

Transition	LDA	GGA
B4 → B1	9.08 (9.02)	11.59 (11.51)
Exp.	9.1[a], 8.7[b]	
Theory	6.60[c], 9.0[d]	9.32[c], 11.8[d]
B1 → B2	268.3 (267.66)	253.2 (252.91)
Theory	260[c]	256[c]
B4 → B_k	27.66 (27.86)	24.35 (24.65)
B_k → B_h	30.50 (30.41)	32.36 (32.93)
B_h → B2	156.90 (156.28)	144.40 (144.77)
B_k → B_i	12.19 (12.13)	16.26 (16.05)
B_i → B2	248.2 (247.9)	213.50 (213.20)
B4 → $B8_1$	17.93 (17.71)	19.60 (19.52)
$B8_1$ → B2	196.05 (195.65)	183.40 (183.27)
B4 → B32	230.20 (229.10)	218.90 (219.10)

[a]Reference 3.
[b]Reference 2.
[c]Reference 6.
[d]Reference 5.

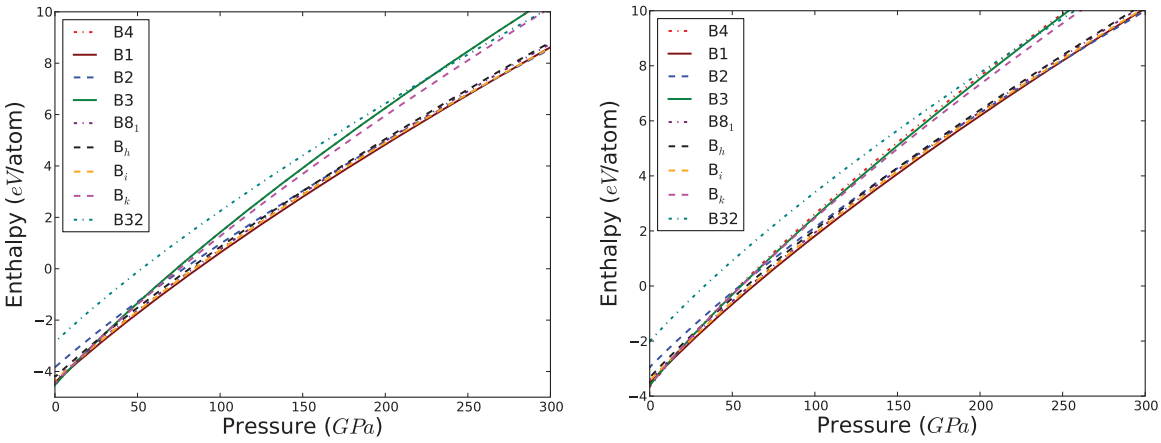

FIG. 3. (Color online) Enthalpy (eV/atom) versus applied pressure (GPa) for the phases of ZnO calculated with the (a) LDA and (b) PBE-GGA functionals.

differ by the stacking in the [001] or [111] direction as pointed out in Refs. 28 and 29.

In agreement with previous theoretical results,[6,12,30] Fig. 1 shows the fact that B4 (wurtzite) is the most energetically stable phase at equilibrium amongst all the phases considered. The NaTl (B32) structure is shown to be less stable than all the other structures at equilibrium. The energy ordering of these phases predicted by both LDA and GGA is $E_{B4} < E_{B3} < E_{B_k} < E_{B1} < E_{B_i} < E_{B8_1} < E_{B_h} < E_{B2} < E_{B32}$, with B4 and B32 phases being, respectively, the most stable and less stable at equilibrium. It is worth noting that most of the phases lie quite close in energy. However, at zero temperature and pressure the other phases may be energetically unlikely.

The ZnO cohesive energy (E_{coh}) was found by subtracting the energy of the isolated constituent atoms from the total energy per ZnO formula unit of the crystal at its equilibrium lattice constant,

$$E_{\text{coh}}(\text{ZnO}) = E_{\text{ZnO}}^{\text{solid}} - \left(E_{\text{Zn}}^{\text{atom}} + E_{\text{O}}^{\text{atom}}\right). \quad (1)$$

The energy calculations for both the isolated atoms and crystal must be performed at the same level of accuracy in order to obtain accurate values for the cohesive energy. The cohesive energy and equilibrium volume are compared with available theoretical results in Table II. The results demonstrate the LDA's tendency to overestimate cohesive energies, while volumes are typically underpredicted. In contrast to LDA, the GGA is known to decrease cohesive energies while overestimating the volumes. On the other hand, we find excellent agreement between our calculated equilibrium volumes and those reported by other workers,[6,31] using both LDA and GGA.

V. PHASE TRANSITION PRESSURES

In Table III, we summarize phase transition pressures obtained by applying the common tangent method on the $E(V)$ equation of state plots of Fig. 1. Here, the negative of the slope $(-dE/dV)$ of the common tangent between two phases quantifies the actual pressure at which one phase transforms to another. Since it is difficult to calculate accurate slopes from common-tangent lines, we also show in Table III transition pressure values determined by computing the Gibbs free energies (G)

$$G = E_{\text{total}} + PV - TS \quad (2)$$

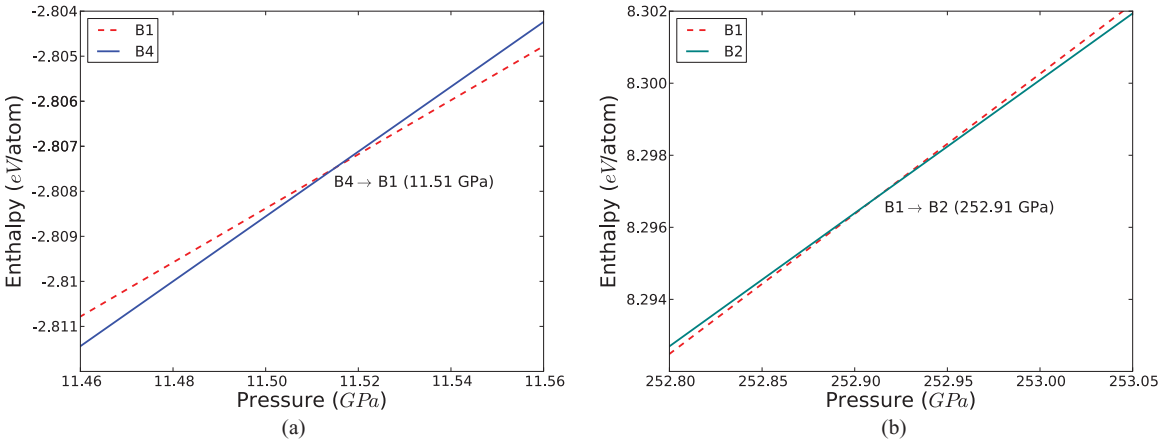

FIG. 4. (Color online) The phase transition pressure regions for the (a) $B4 \rightarrow B1$ and (b) $B1 \rightarrow B2$ phase transitions in the GGA functional.

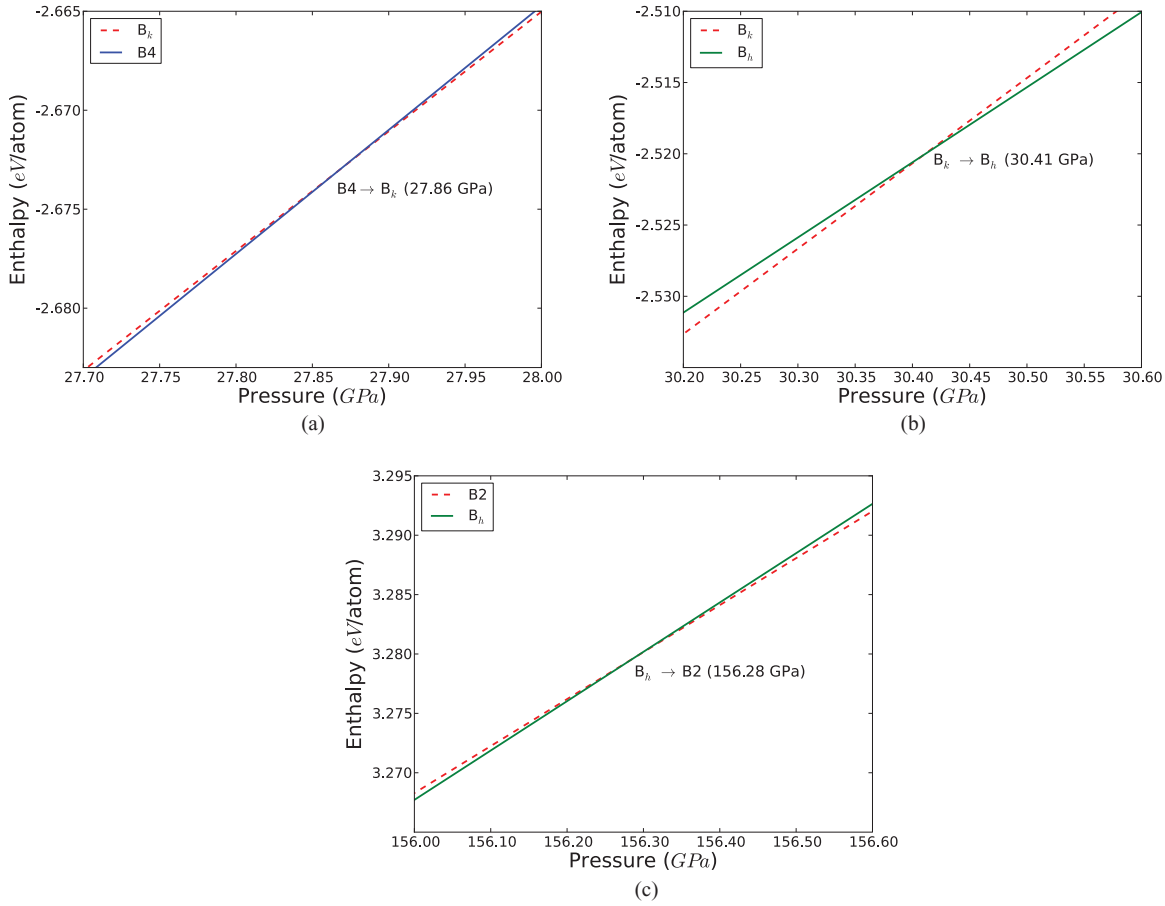

FIG. 5. (Color online) The phase transition pressure regions for the (a) $B4 \rightarrow B_k$, (b) $B_k \rightarrow B_h$, and $B_h \rightarrow B2$ phase transitions in the LDA functional.

for each of the phases. The calculations are performed at zero temperature, and therefore the Gibbs free energy becomes equal to the enthalpy (H)

$$H = E + PV. \tag{3}$$

A stable structure at a given pressure is one for which enthalpy has its lowest value, and thus transition from one phase to another is given by a pressure at which the enthalpies for the two phases are equal. Hence transition pressure values were obtained from the crossing points of the enthalpy versus pressure curves shown in Fig. 3. This procedure gives physically equivalent results to the common tangent method, but it is numerically more accurate. Values from the enthalpy-pressure curves (shown in brackets) agree very well with those obtained from the energy-volume curves. The only available experimental phase transition data in ZnO to date is for the $B4 \rightarrow B1$ transition.

The LDA predicts a transition from the tetrahedraly coordinated B4 to the six-fold coordinated B1 structure at about 9.02 GPa, which falls within the experimental values[2,3] of 8.7 GPa and 9.1 GPa. Although our GGA result (11.51 GPa) for this transition is larger than 9.32 GPa of Ref. 6, it is well in agreement with a similar GGA value of 11.8 GPa reported by Meyer *et al.*[5] The crossover region for this phase transition is shown in Fig. 4(a) for the GGA functional. Above the $B4 \rightarrow B1$ transition, the B1 structure remains stable over a wide pressure range until a transition ($B1 \rightarrow B2$) into the eight-fold coordinated B2 structure is achieved at pressures around 267.66 GPa in the LDA or 252.91 GPa in the GGA [see Fig. 4(b)]. The LDA and GGA pressures for this transition agree to about 5%, suggesting that gradient corrections to the LDA are very small at higher pressures. This agrees fairly well with the LDA and GGA results of Refs. 6 and 12.

The B2 phase has never been observed experimentally, perhaps because pressures around 250 GPa are challenging to reach for static high-pressure experimental techniques.[32] Recent angular dispersive x-ray diffraction experiment by Liu *et al.*[8] has shown that the B1 phase of ZnO remains stable under high pressure up to 209 GPa at room temperature, being the maximum pressure attained in any experiment on ZnO to date.

We predict that the low-pressure B4 phase will transform to the high-pressure B2 phase indirectly, with intermediate phases B_k and B_h as pathway, following the sequence $B4 \rightarrow B_k \rightarrow B_h \rightarrow B2$. These happen at the enthalpy (H) curve crossings, where $H(\mathrm{B4}) = H(\mathrm{B}_k)$, $H(\mathrm{B}_k) = H(\mathrm{B}_h)$ and $H(\mathrm{B}_h) = H(\mathrm{B2})$ at about 27.87 GPa, 30.41 GPa and 156.28 GPa respectively, within LDA. The enlarged regions for this phase sequence are shown on Fig. 5. It has been reported in Ref. 27 that covalent materials transform into the higher coordination structures as pressure increases. However

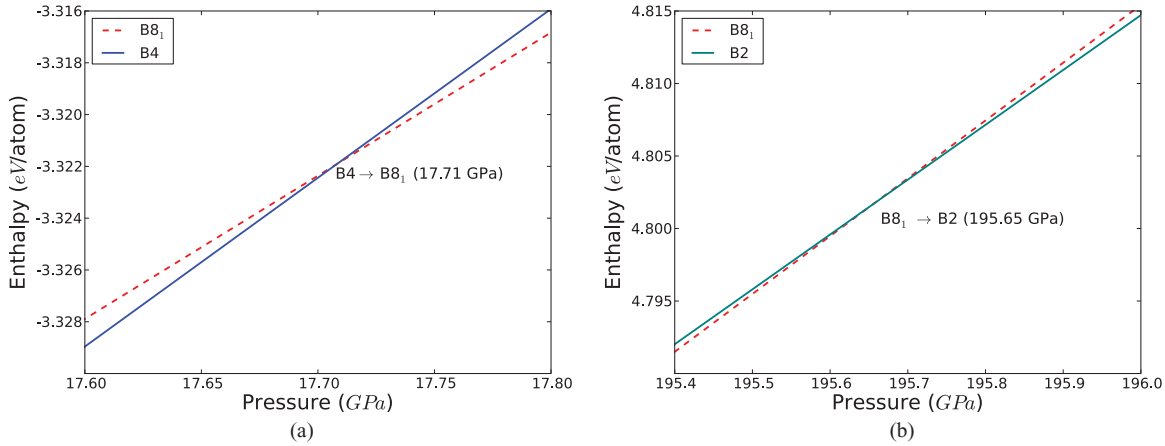

FIG. 6. (Color online) The phase transition pressure regions for the (a) $B4 \rightarrow B8_1$ and (b) $B8_1 \rightarrow B2$ phase transitions in the LDA functional.

we find that the $B4 \rightarrow B_k$ transition is characterized by a decrease in coordination number from four to three. The results also show a possible transition from B_k to B2 phase via the B_i phase, following the order $B_k \rightarrow B_i \rightarrow B2$ with pressures of about 12.13 GPa and 247.9 GPa respectively, within LDA or 16.05 GPa and 213.20 GPa respectively within GGA. Furthermore, application of pressure on the B4 phase causes a transition to B2 phase, with the six-fold coordinated $B8_1$ as the intermediate phase according to the order $B4 \rightarrow B8_1 \rightarrow B2$. It requires a pressure of about 195.65 GPa for a $B8_1 \rightarrow B2$ transition, while about 17.71 GPa is required for the preceding ($B4 \rightarrow B8_1$) transition, according to the LDA as shown in Fig. 6. Lastly, we predict that the B4 phase undergoes a direct transition to the nine-fold coordinated B32 phase at about 229.10 GPa within LDA or 219.10 GPa within GGA.

These results show that the B2 structure is the most preferred candidate for high pressure phases in ZnO among all the structures considered in this study. This phase is most stable at pressures beyond 250 GPa. As already mentioned, the predicted B2 phase has, however, not been verified experimentally so far due to the difficulties in achieving pressures in the vicinity of 250 GPa. When comparing the LDA and GGA results, we find, as in Ref. 6 that the GGA corrects the tendency of the LDA to underestimate transition pressures between low-pressure phases. This behavior is seen in particular for the transitions emanating from the four-fold coordinated B4 and B_k structures, except for the $B4 \rightarrow B32$ phase transition. For high-pressure phases however, the GGA is not consistent as it tends to predict smaller values, suggesting that gradient corrections are unimportant for this material at high pressures. Other than the $B4 \rightarrow B1 \rightarrow B2$ phase transition, there is neither experimental nor theoretical data for the other phase transitions in ZnO, and the results presented here can be considered as predictions.

VI. SUMMARY AND OUTLOOK

First-principles plane-wave calculations have been performed within density functional theory to study the structural phases of ZnO. Both the LDA and GGA were employed within the framework of the PAW method. It has been demonstrated by means of detailed structural phase diagrams, that other structures may exist as candidates for the most stable phase in ZnO. In agreement with previous *ab initio* and experimental studies, our results confirm the wurtzite (B4) structure as the most stable low-pressure phase of ZnO while the hypothetical CsCl (B2) structure is the most favorable high-pressure phase. Apart from the well-documented $B4 \rightarrow B1 \rightarrow B2$ phase transition, this study revealed other transition paths from B4 to B2 structure. In particular, we predicted the phase sequences $B4 \rightarrow B_k \rightarrow B_h \rightarrow B2$ and $B4 \rightarrow B8_1 \rightarrow B2$, with B_k, B_h and $B8_1$ as intermediate phases.

Despite their success in predicting accurate ground state properties, the LDA and GGA are well known to yield a poor account of the band gaps in semiconducting materials. Further examination of the electronic band structure with increasing pressure through the phase transitions would be an interesting extension of the present paper. Methods such as hybrid DFT and GW approximation could offer a better solution in this regard.

ACKNOWLEDGMENTS

We acknowledge support from the National Research Foundation (South Africa), the National Institute for Theoretical Physics, and the University of the Witwatersrand.

*mpmolepo@yahoo.com

[1]C. H. Bates, W. B. White, and R. Roy, Science **137**, 993 (1962).

[2]H. Karzel, W. Potzel, M. Köfferlein, W. Schiessl, M. Steiner, U. Hiller, G. M. Kalvius, D. W. Mitchell, T. P. Das, P. Blaha, K. Schwarz, and M. P. Pasternak, Phys. Rev. B **53**, 11425 (1996).

[3]S. Desgreniers, Phys. Rev. B **58**, 14102 (1998).
[4]M. Kalay, H. H. Kart, S. Ozdemir Kart, and T. Cagin, J. Alloys Compd. **484**, 431 (2009).
[5]B. Meyer and D. Marx, Phys. Rev. B **67**, 035403 (2003).
[6]J. E. Jaffe, J. A. Snyder, Z. Lin, and A. C. Hess, Phys. Rev. B **62**, 1660 (2000).
[7]J. Serrano, A. H. Romero, F. J. Manjon, R. Lauck, M. Cardona, and A. Rubio, Phys. Rev. B **69**, 094306 (2004).
[8]H. Liu, J. Tse, and H. Mao, J. Appl. Phys. **100**, 093509 (2006).
[9]W. Kohn and L. J. Sham, Phys. Rev. **140**, A1133 (1965).
[10]J. P. Perdew, K. Burke, and Y. Wang, Phys. Rev. B **54**, 16533 (1996).
[11]P. Hohenberg and W. Kohn, Phys. Rev. **136**, B864 (1964).
[12]J. Uddin and G. E. Scuseria, Phys. Rev. B **74**, 245115 (2006).
[13]Y. Saeed, A. Shaukat, N. Ikram, and M. Tanveer, J. Phys. Chem. Solids **69**, 1676 (2008).
[14]B. Amrani, I. Chiboub, S. Hiadsi, T. Benmessabih, and N. Hamdadou, Solid State Commun. **137**, 395 (2006).
[15]A. Zaoui and W. Sekkal, Phys. Rev. B **66**, 174106 (2002).
[16]Y. Azzaz, S. Kacimi, A. Zaoui, and B. Bouhafs, Physica B **403**, 3154 (2008).
[17]Z. Li, Y. Xu, G. Gao, T. Cui, and Y. Ma, Phys. Rev. B **79**, 193201 (2009).
[18]G. Kresse and J. Hafner, J. Phys. Rev. **47**, 558 (1993).
[19]G. Kresse and J. Hafner, J. Phys. Condens. Matter **6**, 8245 (1994).
[20]D. M. Ceperley and B. J. Alder, Phys. Rev. Lett. **45**, 566 (1980).
[21]J. P. Perdew and A. Zunger, Phys. Rev. B **23**, 5048 (1981).
[22]P. E. Blöchl, Phys. Rev. B **50**, 17953 (1994).
[23]G. Kresse and D. Joubert, Phys. Rev. B **59**, 1758 (1999).
[24]H. J. Monkhorst and J. D. Pack, Phys. Rev. B **13**, 5188 (1976).
[25]G. Kresse and J. Furthmüller, *VASP the GUIDE* (Universität Wien, Wien, Australia, 2005).
[26]F. Birch, Phys. Rev. **71**, 809 (1947).
[27]S. Limpijumnong and S. Jungthawan, Phys. Rev. B **70**, 054104 (2004).
[28]Roberto J. Guerrero-Moreno and Noboru Takeuchi, Phys. Rev. B **66**, 205205 (2002).
[29]A. Schleife, F. Fuchs, J. Furthmuller, and F. Bechstedt, Phys. Rev. B **73**, 245212 (2006).
[30]J. E. Jaffe and A. C. Hess, Phys. Rev. B **48**, 7903 (1993).
[31]J. Wróbel and J. Piechota, Phys. Status Solidi B **244**, 1538 (2007).
[32]H. Liu, H. K. Mao, M. Somayazulu, Y. Ding, Y. Meng, and D. Hausermann, Phys. Rev. B **70**, 094114 (2004).